Impact of Asphalt Mixture Specification Limits: A Theoretical Analysis

Filippo G Pratico, Armando Astolfi, Domenico Vizzari, Giuseppe Colicchio

Author manuscript accepted published in Journal of Materials in Civil Engineering, 32, (5), 2020. ASCE
https://doi.org/10.1061/(ASCE)MT.1943-5533.0003116

The Impact of Asphalt Mixture Specification Limits: A Theoretical Analysis

Author

Filippo G. Praticò
Associate Professor, DIIES Department, University Mediterranea of Reggio Calabria, Italy (corresponding author).
E-mail: filippo.pratico@unirc.it

Armando Astolfi
Ph.D Student, DICAM Department, University of Palermo, Italy.
E-mail: armandoastolfi@gmail.com

Domenico Vizzari
PhD Student, IFSTTAR, Route de la Bouaye - 44340 Bouguenais – Nantes, France.
E-mail: domenico.vizzari@ifsttar.fr

Giuseppe Colicchio
Professional Engineer, DIIES Department, University Mediterranea of Reggio Calabria, Italy.
E-mail: giuseppe.colicchio@unirc.it

Abstract

Specifications limits and tolerances are crucial in the relationships among contractor, road agency, and citizens, because they impact profits, acceptance procedures, and pavement durability. They mainly depend on processes involved and unfortunately their relationship with durability is mainly empirical and calls for further investigation. In the light of the above, the study described in this paper deals with assessing how durability and pay adjustment are affected by variations of the explanatory variables (e.g., air void content) within specification limits. A model was set up in order to assess the impact on the modulus of a bituminous mixture, which is a crucial factor for the expected life. The model was applied to a well-known set of contract specifications, in order to check for their suitability and rationale. Results demonstrate that, usually, air void-related consequences are worse than penetration-related consequences, which, in turn, outrank aggregate gradation and asphalt content-related consequences. An exception is given by the maximum size of aggregates. Furthermore, when pay adjustments build on empirical algorithms, they have to be layer-specific because the same "error" implies severer consequences in deeper layers. Results can benefit both researchers and practitioners.

Introduction

The dynamic modulus of a bituminous mixture (supposed to act as a linear viscoelastic material) is a complex number and is an important parameter in the design procedure because it affects the expected life of asphalt pavements (Colonna et al., 2012; Clyne et al. 2003). Its absolute value is calculated as the peak stress amplitude (σ_o) divided by the peak amplitude of recoverable axial strain (ε_o, cf. NCHRP Report 465). Stress and strain distribution depend on moduli. Importantly, the impact of modulus on expected life is multifaceted because many other parameters affect these relationships: 1) higher moduli may correspond to lower strains (Shahadan et al., 2013); 2) at the same time they may correspond to lower fatigue cracking performance; 3) furthermore, lower performance to thermal cracking is expected.

Many authors have proposed algorithms to estimate the dynamic modulus based on nonlinear regressions, semi-empirical methods or rheological models. Input data are typical asphalt mixture parameters that refer to volumetric properties, aggregate gradations, test conditions (i.e. temperature and loading frequency) and asphalt binder (i.e. viscosity and percentage).

Among the models in the literature, the following can be listed:

i. Nielsen Model, 1970 (Nielsen 1970, Riccardi 2017), based on mortar characteristics (fine aggregates + bitumen);
ii. Asphalt Institute, 1982 (Asphalt Institute 1982, Giuliana et al. 2011);
iii. Witczak - NCHRP 1-40D model, 1996 (Witczak and Fonseca1996, Yu 2012, Riccardi 2017) or Witczak-ban model, where the dynamic shear modulus and the phase angle of the asphalt binder are used;
iv. Witczak 1-37A model, or Witczak-Andrei model, 1999 (Andrei et al. 1999, Yousefdoost et al. 2013, cf. eq. 1);
v. Hirsch Model, 2002 (Christensen et al. 2015, Riccardi 2017), that is based on VMA, VFA and G_b;
vi. Lee et al. 2002, based on Witczak 1-37A model;
vii. Alkhateeb Model, 2006 (Alkhateeb et al. 2006, Yousefdoost et al. 2013), that involves voids of mineral aggregates, VMA, and the shear modulus of the asphalt binder, G_b;
viii. Cho et al., 2010, where the dynamic modulus is a function similar to the one of the Witczak 1-37A model, but depends linearly on ρ_{200} (Cho et al. 2010, Georgouli et al. 2016);

ix. Seo et al., 2013, based on Witczak 1-37A model and FWD data;

x. Leiva-Villacorta et al. 2013, based on artificial neural networks and on Witczak 1-37A model;

Note that they basically refer to four main families: Nielsen, Asphalt Institute, Hirsch, and Witczak.

The 1999 Witczak model (1-37A, Yu 2012) is based on nonlinear regressions, derived by analyzing 205 laboratory mixtures (171 unmodified asphalt binders and 34 modified binders), for a total of 2750 data points. The model predicts the dynamic modulus E* (psi) of HMA mixtures based on eight main input parameters that describe loading condition, aggregate gradation, asphalt binder characteristics and interaction with aggregates.

$$\log\left|E^*\right| = 3.750063 + 0.02932 \cdot \rho_{200} - 0.001767 \cdot (\rho_{200})^2 - 0.002841 \cdot \rho_4 - 0.058097 \cdot AV + \\ - 0.802208 \cdot \left(\frac{V_{beff}}{V_{beff} + AV}\right) + \frac{3.871977 - 0.0021 \cdot \rho_4 + 0.003958 \cdot \rho_{3/8} - 0.000017 \cdot (\rho_{3/8})^2 + 0.00547 \cdot \rho_{3/4}}{1 + e^{(-0.603313 - 0.313351 \cdot \log(f) - 0.393532 \cdot \log(\eta))}} \quad (1)$$

In the equation above, |E*| is the absolute value of the dynamic modulus [psi], (1psi = 0.0069MPa], η is asphalt binder viscosity [10 Poise = 1 Pas], *f* is the loading frequency [Hz], AV is the air void content [%], V_{beff} is the effective asphalt binder content [% by volume], $\rho_{3/4}$ is the cumulative % retained on the 19 mm (3/4 inch) sieve, $\rho_{3/8}$ is the cumulative % retained on the 9.5 mm (3/8 inch) sieve, ρ_4 is the cumulative % retained on the 4.75 mm (No. 4) sieve, and ρ_{200} is the percentage passing through the 0.075 mm (No. 200) sieve.

For the viscosity, it can be assessed based on experiments or it can be predicted through models, such as the one below (Yu 2012):

$$\log(\eta) = 10.5012 - 2.2501 \cdot \log(Pen) + 0.00389 \log(Pen)^2 \quad (2)$$

Where η is the viscosity [Poise], Pen [0.1mm] refers to the penetration of a standard needle of 100 g, which penetrates the asphalt binder for 5 seconds.

Even if modulus derivation is a complex topic (Garcia and Thompson 2007, Cross at al. 2007, Esfandiarpour and Shalaby 2017, Praticò et al. 2016), Witczak model is an excellent solution for a given real mixture but, for the purpose of this paper, it is not possible to consider input parameters as "independent". Indeed, changing a

single variable implies variations on other input parameters (i.e., explanatory variables). In particular: i) aggregate gradation ($\rho_{3/4}$, $\rho_{3/8}$, ρ_4 and ρ_{200}) influences bulk specific gravity and apparent specific gravity of aggregates (G_{sb} and G_{sa}); ii) asphalt content (P_b) and asphalt binder specific gravity (G_b) influence the percentage of absorbed asphalt (P_{ba}), the volume of absorbed asphalt binder (V_{ba}), the effective asphalt content (P_{be}), and the volume of effective asphalt binder content (V_{beff}); iii) P_b and G_b influence the maximum theoretical specific gravity of the mixture (G_{mm}). For example, a variation of asphalt content or of the passing ρ_{200} implies a change of the air voids and consequently of the dynamic modulus.

Based on the above, the reciprocal relationships among the explanatory variables cannot be overlooked for a proper modulus estimation.

Objectives

In the light of the issues above, the study described in this paper aims at studying the effect of the variation of the main contract variables (e.g., ρ_{200}) within the range permitted by contract specifications and tolerances. This includes: i) assessing the effects on moduli, expected life and pay adjustment, based on the synergistic consideration of the mutual effects among the different explanatory variables which impact estimation models; ii) Proposing and applying a criterion for deriving specification limits well-grounded in logic.

The main tasks of this study were the following:

- Task 1: Modelling (section below). In this task, due to the interdependency among several variables of the algorithm for the derivation of moduli, a model was set up to derive the value of G_{mb} based on a number of inputs.
- Task 2: Derivation and discussion of model outputs. In this task, the derivation of mechanistic properties, expected life and pay adjustment was carried out as a function of each contract variable. Based on the equations set up, consequences in terms of pay adjustment were inferred.
- Task 3: Conclusions and recommendations (last section). In this task, analyses were carried out and recommendations were derived.

Modelling

The Flow chart in Fig. 1 illustrates the conceptual framework to derive a layer modulus. In more detail, the synergistic effect of gradation percentages and construction on volumetrics is depicted. It summarizes the path towards the derivation of the modulus of a layer in terms of the Witczak model and clearly illustrates that multiple phenomena of linear or non-linear correlations between couples of explanatory variables are present (risk of multicollinearity). For example, P_b affects both V_{beff} and AV, which are inversely correlated.

Apart from the quality characteristics of asphalt binder (Pen, η) and load frequency, gradation affects ρ_i, G_{sb}, as well as G_{sa} and G_{se}. This latter affects G_{mm} (together with P_b and G_b). G_{mb} depends on G_{mm}, on P_b, and on compaction effort (N). From G_{mm} and G_{mb}, AV can be derived, while based on P_b, G_b, and stone specific gravities (G_{sb}, G_{se}, G_{sa}), absorbed (V_{ba}, P_{ba}) and effective asphalt binder (V_{eff}, P_{be}) can be derived.

The main relationships among the explanatory variables of Witczak model are summarized below (symbols are explained in Fig. 1). Equations below refer to gradation and specific gravity (Sukirman 2010, Arifin et al. 2015, McGennis et al. 1995):

$$\rho_{3/4} = 100 - P_{19mm} \tag{3}$$

$$\rho_{3/8} = 100 - P_{9.5mm} \tag{4}$$

$$\rho_4 = 100 - P_{4.75mm} \tag{5}$$

$$G_{sb} = \frac{\sum_{i=1}^{n} P_i}{\sum_{i=1}^{n} \frac{P_i}{G_i}} \tag{6}$$

$$G_{se} = G_{sb} + cf \cdot (G_{sa} - G_{sb}) \tag{7}$$

P_s-P_b volumetric parameters follow the well-known relationships (Al-Khateeb et al. 2006, California Test Number 2010, and WAQTC TM 13 2012):

$$P_s = 1 - P_b \tag{8}$$

$$G_{mm} = \frac{1}{(\frac{P_s}{G_{se}}) + (\frac{P_b}{G_b})} \quad (9)$$

$$P_{ba} = \frac{G_{se} - G_{sb}}{G_{sb} \cdot G_{se}} \cdot G_b \quad (10)$$

$$V_{ba} = \frac{\frac{P_{ba} \cdot P_s}{100}}{G_b \cdot G_{mb}} \quad (11)$$

$$V_{ba} = \frac{100 \cdot P_s \cdot \frac{1 - G_{se}}{100}}{\frac{P_b}{100} \cdot G_b + \frac{P_s}{100} \cdot G_{se}} \cdot 100 \cdot \left(\frac{1}{G_{sb}} - \frac{1}{G_{se}} \right) \quad (12)$$

$$P_{be} = P_b - P_{ba} \cdot P_s \quad (13)$$

$$V_{beff} = \frac{P_{be} \cdot G_{mb}}{G_b} \quad (14)$$

$$AV = \frac{G_{mm} - G_{mb}}{G_{mm}} \quad (15)$$

$$VMA = 100 - \frac{G_{mb} - P_s}{G_{sb}} \quad (16)$$

$$VFA = \frac{VMA - AV}{VMA} \cdot 100 \quad (17)$$

$$VFA = \frac{\frac{P_{be}}{G_b}}{\frac{VMA}{G_{mb}}} \cdot 100 \quad (18)$$

It is worth noting that equations above depend on G_{mb}. This latter should be measured on the given bituminous mixture of given G_{se}, G_b, P_b.

For G_{mb}, based on the literature, two main synergistic effects must be considered, i.e., compaction and asphalt binder content. Low P_b values do not permit a proper lubrication of particle contacts. It follows that a proper packing is hindered and G_{mb} is reduced.

Higher asphalt binder contents allow optimizing the packing of particles and achieving higher values of G_{mb}. If P_b exceeds a given optimal content, the lubrication effect is not anymore the most relevant factor because the excessive amount of asphalt binder tends to decrease the overall G_{mb} and G_{mm}, which both tend towards G_b.

At the same time, for a given asphalt content, higher compaction efforts imply higher G_{mb} and lower air voids content, AV.

Compaction efforts (e.g., number of passes) do not increase the G_{mb} indefinitely, this latter approaching a given asymptotic value.

Based on the above, from a predictive standpoint, the following equation is herein set up:

$$G_{mb} = \left[a\left(\frac{P_b}{100}\right)^2 + b\left(\frac{P_b}{100}\right) + c \right] \cdot \left[d + (1-d)\exp(N\% - 1) \right] \quad (19)$$

Where a, b, c and d are coefficients to calibrate, N% is the compaction energy expressed in terms of number of passes with respect to the "refusal" value (it ranges from 0 to 1). The factor containing P_b refers to the effect of bitumen percentage on specific gravity. The factor containing d refers to compaction and ranges from 0 to 1. Consequently, d ranges from $-[\exp(1)-1]^{-1}$ to 1. For a given P_b, AV tends to its maximum value when N% tends to 0. In contrast, AV tends to its minimum, when N% tends to its maximum (1).

In Fig. 2 a dense-graded mix (Bulletin 27) and an open-graded mix containing ferrite (Peinado et al. 2014) are fitted through equation 19.

Based on the synergistic derivation of the volumetric indicators, moduli were derived through eq. (1) (Cf. Fig. 1, Yu 2012).

Poisson coefficients were derived based on the literature (Rojas et al. 1998, Popovics 2008, Maher and Bennert 2008, Xiao 2009, Pezzano 2009, Houben 2009, Jung et al. 2012, Ghadimi et al. 2013, Hanifa et al. 2015).

For the derivation of the expected life, the software KenLayer was used (Huang 2004). This software analyzes pavements based on multi-layer elastic theory under a circular loaded area. KenLayer can be applied to layered systems under single, dual, dual-tandem, or dual-tridem wheels. To analyze pavements using KenLayer software, the inputs required are section, geometry, material properties and wheel load. The main outputs are stresses, deflections, and design life. Damage analysis can be made by dividing each year into a maximum of 12 periods, each with a different set of material properties. The geometry and moduli of the pavement are reported in Fig. 3 and Table 1 and, in order to obtain an as-design life of 20 years, a traffic load of about 15 million TNRL (total number of load repetitions for each load group during each period) is considered.

Authors are aware of: 1) the dependence of outputs on traffic configurations, pavement structures, and local environment; 2) the dependence of moduli on the given algorithm; 3) the existence of different versions of the Witczak model, intended to adapt this latter to porous asphalt concretes (Giuliana et al. 2011, Geourgouli et al. 2016).

To this end, it is worth noting that the analyses carried out in this study aim at highlighting the impact of specification limits on expected life under given hypotheses.

Cost Modelling

The expected life is a key-factor in the Life Cycle Cost Analyses (LCCA or LCC) of the pavement. LCCA is a process for evaluating the total economic worth of a usable project segment by analyzing initial costs and discounted future cost, such as maintenance, user, reconstruction, rehabilitation, restoring, and resurfacing costs, over the life of the project segment (Walls and Smith 1998). Minimizing the pavement life cycle costs will increase the sustainability of the pavement system (Praticò 2016). LCCA includes agency costs (AC), which include initial preliminary engineering, contract administration, construction supervision and construction costs, as well as future routine and preventive maintenance, resurfacing and rehabilitation costs, salvage values, and sunk costs.

ACs affect the present value (PV) of agency costs (i.e. the future amount of expenses, discounted to reflect the current value, Praticò 2016). The difference between the PV referred to the rehabilitation works of the design pavement and the PV referred to the modified pavement (i.e., changing percentage of mix aggregates, percentage of asphalt binder or its penetration) is the pay adjustment (PA), which is defined as “the actual

amount, either in dollars or in dollars per area/weight/volume, which is to be added or subtracted to the contractor's bid price or unit bid price" (Hughes et al. 2011).

For PV, the following equations were applied:

$$PV_{REH} = C_{REH} \frac{\left(R^{D} - R^{EXL}\right)}{1 - R^{D}} \quad (20)$$

$$PV_{RES} = C_{RES} \frac{R^{O}}{1 - R^{D}} \quad (21)$$

Where:

- R is the ratio between (1+i) and (1+r), where, for example, i=0.04 (inflation rate) and r=0.08 (interest rate).
- C_{REH} refers to costs occurred in successive rehabilitations [€/m^2].
- C_{RES} refers to costs occurred in successive resurfacings [€/m^2].
- D is the expected life of the as-design pavement [years]. In more detail, D is the minimum expected life of the different layers of the pavement. D does not take into consideration the friction course (which will usually undergo its failure in a time that is smaller than D);
- EXL=EREH is the expected life of the as-constructed pavement [years]. EXL corresponds to D (but it refers to the as-built pavement), in the sense that EXL does not take into consideration what happens to the friction course;
- O=EXLFC=ERES is the expected life of the as-constructed friction course [years]. In other words, it is the time between two successive resurfacings (FC, typically 10 years).

In the next figures (results of the analysis), the ratios PA_{REH}/C_{REH} and PA_{RES}/C_{RES} were used. If these ratios are positive, they represent a bonus. If not, they represent a penalty. Finally, it is worth pointing out that: 1) in this case, due to the nature of the simulation (carried out on the "boundaries", specification limits), random sampling through Monte Carlo simulation was not used (Wu et al. 2017). 2) even if pay factors based on expected life are complex to apply, their use is here needed in the pursuit of objectives.

Simulations and discussion

In the pursuit of the objectives stated above, the pavement structure in Fig. 3 and Table 1 was considered (As-Design Pavement). Additionally, in Table 1, reference moduli and thicknesses gathered from the literature are reported.

Friction Course (FC)

This section deals with the effects deriving from the variation of the main characteristics of FC (Porous Asphalt Concrete, PAC, cf. Fig. 4 to Fig. 6).

X-axes refer to the parameter under investigation (i.e., parameter which is supposed to vary in a certain range but that may undergo variations outside the specification limits).

Y-axes refer: i) to the expected life of the pavement, EXL (i.e., by referring to rehabilitations). Usually the cement-treated base course was the cause of the pavement failure; ii) to the pay adjustment of the pavement (part referred to rehabilitations, PA_{REH}) expressed as a percentage of the corresponding cost (C_{REH}), i.e., PA_{REH}/C_{REH}, eq. (20). It is noted that for the case under investigation C_{REH} includes the cost of friction course, binder course, base course, and cement-treated base course; iii) to the pay adjustment for resurfacing (PA_{RES}), expressed as a percentage of the corresponding cost (C_{RES}), i.e., PA_{RES}/C_{RES}, eq. (21). Note that C_{RES} refers to the cost of the FC.

$P_{3/4}$ (Fig. 4-A) refers to the passing through the 3/4-inch sieve, which corresponds to 100-$\rho_{3/4}$, where $\rho_{3/4}$ is the cumulative percentage retained on the 19 mm (3/4 inch) sieve (cf. eq. 1).

Note that the default value is $P_{3/4}$=100, which corresponds to an EXL of 20 years and to a PA% of zero. Lower values imply higher expected lives (Fig. 4-A, left y-axis) and then positive PAs (<1%, Cf. Fig. 4-A, right y-axis).

Fig. 4-B refers to the effects of nonconformities of $\rho_{3/8}$ (9.5mm sieve), where the default value is $P_{3/8}$= 37.5% (that corresponds to a value of 62.5% for ρ_{38} and to EXL=20, PA_{REH}=0%, PA_{RES}=0%). Higher values imply a reduction of the expected life (negative PA_{REH} and PA_{RES}), while lower values may imply an increase ($P_{3/8}$≈13-20) or a relative decrease ($P_{3/8}$≈20-38, approximately). Note that if $P_{3/8}$ is higher than about 20% (and lower

than the default value) PA_{REH} and PA_{RES} are positive (bonus), while for $P_{3/8}$ close to 20%, both PA_{REH} and PA_{RES} approach a maximum (optimal condition).

Fig. 4-C focuses on ρ_4 (4.76 mm sieve) with a default value of P_4=18.5% (that corresponds to a cumulative % retained of 81.5 for ρ_4). Higher values of P_4 (>18.5%) imply an increase of expected life, PA_{REH}, and PA_{RES}. Instead, for lower values of P_4 (< 18.5%), expected life, PA_{REH}, and PA_{RES} are reduced.

Fig. 5-A refers to the effects of nonconformities of ρ_{200} (% passing through the 0.075 mm sieve), with a default value of P_{200}=ρ_{200}=10%.

Expected life, PA_{REH} and PA_{RES} have a "weak" parabolic behavior, with maxima corresponding to 8%. It is interesting to note that for passing percentages higher than 18%, the expected life shows a sharp reduction, with values of 0.1 years. This type of nonconformity corresponds to the failure of the friction course.

Fig. 5-B refers to the effects of asphalt binder penetration, where the default value is 60 (0.1 mm).

Expected life, PA_{REH}, and PA_{RES} have a nonlinear behavior. In particular, for penetrations higher than 60, the expected life is lower and PA_{REH} and PA_{RES} have a negative sign. On the contrary, for penetrations lower than 60, the expected life is higher and PA_{REH} and PA_{RES} become positive.

Fig. 5-C focuses on asphalt binder percentage and its effect on expected life (y-axis, left), PA_{REH}% (y-axis, right), and PA_{RES}% (y-axis, right). Note that asphalt binder percentages higher than the default value (=4.76) imply higher EXL and positive PAs, and *vice versa*. Importantly, the model seems to underestimate rutting and plastic deformations for asphalt binder percentages which exceed 8÷10%.

Fig. 6-A illustrates the EXL and the PA compared to air voids (AV). The curves are monotonically decreasing and higher values of AV imply lower values of EXL and of PA. In particular, for AV higher than about 22%, pavement failure is due to the breaking of the friction course. Instead, for AV close to 7%, the failure occurs in the base course.

Binder Course (BIC)

This section deals with effects (on the pavement) caused by BIC characteristics (Figures 4-6).

Fig. 4-D refers to 100-$\rho_{3/4}$ = $P_{3/4}$.

In the case of the BIC, the default $P_{3/4}$ is 78%. Higher values of passing (> 78%) imply a reduction of expected life, of PA_{REH}, and PA_{RES}. Instead, for lower values (< 78%), the expected life, PA_{RES}, and PA_{RES} are higher.

Fig. 4-E focuses on 9.51 mm sieve, with a default value of 57.5% (that corresponds to a cumulative % retained of 42.5 for $\rho_{3/8}$). Unlike the case of the friction course, the behavior of the expected life, of PA_{REH}, and PA_{RES} is linear and without maxima. In particular, higher values (> 57.5%) imply a reduction of expected life, PA_{REH}, and PA_{RES}. Instead, for lower values (< 57.5%), the expected life, PA_{RES}, and PA_{REH} are higher.

Fig. 4-F focuses on P_4 (4.76 mm sieve) with a default value of 42.5% (that corresponds to a cumulative % retained of 57.5 for ρ_4). The linear behavior of expected life, PA_{REH}, and PA_{RES} is similar to the one for the case of the friction course, where higher values of passing (> 42.5%) imply the increase of expected life, PA_{REH}, and PA_{RES}. Instead, for lower values (< 42.5%), EXL, PA_{RES}, and PA_{RES} decrease.

Fig. 5-D refers to the effects of nonconformities of ρ_{200} (0.075 mm sieve), where the default value is 6 %. Expected life, PA_{REH} and PA_{RES} have a parabolic behavior, with maxima corresponding to 8%. In particular, in the range 6-10%, EXL is higher than 20 years, and PA_{REH} and PA_{RES} are positive. In contrast, in 0-6% and 10-16%, EXL decreases, while PA_{REH} and PA_{RES} are negative.

Fig. 5-E refers to the effects of asphalt binder penetration, where the default value is 90 (0.1 mm). Expected life, PA_{REH} and PA_{RES} have a trend that is similar to the one of the friction course (Fig. 5-B).

Fig. 5-F refers to the variation of the asphalt binder percentage, with a default value of 4.5%. For a value of P_b higher than 1.5%, the expected life varies in the range 16-21 years. Instead, for a P_b lower than 1.5%, expected life and pay adjustment have a sharp reduction.

Regarding the binder course (see Fig. 6-B), the trend of EXL and PA with respect to the air void is similar to the one observed for the friction course, with a monotonically decreasing behavior. It is interesting to note that for values of AV higher than 18% the failure of the pavement is due to the BIC. In contrast, if AV is in the range 12.5-18%, the BAC undergoes a premature failure. Finally, if AV is lower than 12.5%, the failure is due to the cement-treated course (CT).

Base Course (BAC)

Fig. 4-G focuses on $\rho_{3/4}$ (100-$P_{3/4}$). In the case of BAC, the default value of the percentage passing through the 19 mm sieve is 72% and the behavior is similar to the one of BIC.

Fig. 4-H refers to $P_{3/8}$ (9.51 mm sieve) with a default value of $P_{3/8}$=52.5% (that corresponds to a cumulative % retained of 47.5 for $\rho_{3/8}$). Like the case of the friction course, the behavior of the expected life, of PA_{REH}, and PA_{RES} is nonlinear with maxima at 45.5%.

Fig. 4-I focuses on 4.76 mm sieve with a default value of P_4=40 % (that corresponds to a cumulative % retained of 60 for ρ_4) and the linear behavior of expected life, PA_{REH}, and PA_{RES} is similar to the one of the friction course and of the binder course.

Fig. 5-G refers to the effects of nonconformities of ρ_{200} (0.075 mm sieve), where the default value is 5.5%. Expected life, PA_{REH}, and PA_{RES} have a parabolic tendency, with maxima corresponding to 8%.

Fig. 5-H focuses on the effects of asphalt binder penetration, with a default value of 90 (0.1 mm).

Expected life, PA_{REH} and PA_{RES} have a nonlinear behavior with maxima at about 70. It is interesting to note that between 50 and 70, PA_{REH}, and PA_{RES} increase. In contrast, for penetrations higher than 90, expected life, PA_{REH} and PA_{REH} decrease and the damaged layer is the CT (PA_{REH} and PA_{REH} are negative). For penetrations in the range 70-90, EXL decreases but PA_{REH} and PA_{RES} are positive and the failure is still occurring in the base course.

Fig. 5-I refers to the variation of the asphalt binder percentage. For a value of P_b higher than 2%, the expected life varies into the range 16-21 years. In contrast, for a value of P_b lower than 2%, expected life and pay adjustment have a sharp reduction.

Fig. 6-C refers to the effect of air voids on EXL and on PA. The trend shows a maximum corresponding to AV=4.5%. In particular, for AV between 1.7% and 4.5%, EXL and PA increase and the pavement failure is due to the BIC. When AV is in the range 4.5-12.2%, EXL and PA decrease and the failure occurs in the CT. Finally, if AV is higher than 12.2%, EXL and PA continue to decrease, but the pavement failure is due to the BAC.

It seems relevant to observe that in some cases EXL has a convex behavior instead of a linear one (e.g., BIC penetration). This happens, for example, when considering the consequences deriving from nonconformities of asphalt binder penetration in BIC or in BAC (cf. Fig. 5-E and Fig. 5-H, respectively).

The rationale behind this convexity is a change in the layer that prematurely fails.

For example, Fig. 7 (A and B) illustrates how the EXL of the pavement (y-axis, which usually derives from the EXL of the deep layers, e.g., unbound base, CT, and BAC) varies when there is a defect of the grade of the asphalt binder (x-axis), with respect to the as-design value (6mm for the FC, 9mm for BAC and BIC).
X-axes refer to the difference between real and as-design penetration.
Fig. 7 (A and B) points out a different behavior for low values of penetration: linearity, in the case of the binder course (Fig. 7-B, BIC), versus convexity in the case of the base course (Fig. 7-A, BAC).
The rationale behind the difference above is that very low penetration values in the BAC imply a premature failure of BAC over CT (see Fig. 7-A). In turn, this fact implies the transition from the straight line of the CT to the straight line of the BAC, which implies the convexity. Importantly, this does not happen for the BIC and for the FC.

Sensitivity analysis

The analysis of the sensitivity of longevity and costs with respect to the variations of the primary variables is here carried out through two innovative parameters (cf. Fig. 8 and Table 2).
To this end, note that the expected life of the pavement, EXL, varies when the given indicator (or explanatory variable, e.g., AV), varies between the upper and the lower specification limits (USL, LSL, respectively); for example:

$$EXL = EXL(AV) \tag{22}$$

As is well known, two types of specification limits can be pointed out: i) LSL_{JMF} and USL_{JMF}, i.e., lower and upper specification limit referred to the job mix formula (e.g., 4.75% and 5.25% in terms of asphalt binder percentage); ii) LSL_{specs} and USL_{specs}, i.e., lower and upper specification limit referred to contract requirements specifications for the given layer (e.g., 4.5% and 5.5%, in terms of asphalt binder percentage).
Usually, LSL_{specs} and USL_{specs} are very general and are a starting point for the job mix formula and for the corresponding LSL_{JMF} and USL_{JMF}.

Table 2 refers to the consequences of the variations of the given indicator, (e.g., AV) within the specification limits, expressed through two parameters herein setup, i.e., ΔY (in terms of years) and ΔPA (in terms of pay adjustment). ΔY is the maximum variation of the expected life (years) of the pavement, for a given couple of specification limits (LSL, USL) of the given indicator. For example:

$$\forall I \in (LSL,\ USL)\ \ \Delta Y = \max EXL - \min EXL \tag{23}$$

Furthermore, ΔPA is defined as follows:

$$\Delta PA = \left|\max(AV) - \min(AV)\right| \tag{24}$$

ΔPA expresses the sensitivity of the ratio PA/C (where PA/C= $(PA_{RES}+PA_{REH})/(C_{RES}+C_{REH})$, [%]) to possible variations in the given indicator (e.g., AV). It depends on the corresponding gap in terms of expected lives.

Table 2 summarizes the results (ΔY and ΔPA) obtained by considering variations of gradation ($\rho_{3/4}$, $\rho_{3/8}$, ρ_4, ρ_{200}), asphalt content (P_b), asphalt binder penetration (Pen), or air voids content (AV), for each single bituminous layer (FC, BIC, or BAC). Table 2 summarizes the results obtained for ΔPA and ΔY.

For example, if the AV of BAC varies in the range 5.5 ± 2.5 %, then this implies variations lower than 1.71 years (EXL) and lower than 5.60% (PA/C).

By referring to the accepted range of variation with respect to the job mix formula (i.e., LSL_{JMF}, USL_{JMF}), note that negligible consequences are expected in terms of both expected life (< 1 year) and PA/C (< 3%). Indeed, for SL_J, based on results in Table 2, note that: i) for nonconformities of $\rho_{3/4}$, $\rho_{3/8}$, ρ_4 for the deepest bituminous layer, BAC, ΔY ranges from 0.43 to 1.10 years; ii) For $\rho_{3/4}$, $\rho_{3/8}$, ρ_4 and for BIC, ΔY ranges from 0.16 to 0.36 years; iii) For $\rho_{3/4}$, $\rho_{3/8}$, ρ_4 and for FC, ΔY ranges from 0.06 to 0.16 years; iv) for ρ_{200}, the sensitivity ranges from 0.11 to 0.73, as a function of the layer involved; v) P'_b has similar consequences.

By referring to the accepted range of variation with respect to the general contract (LSL_{specs}, USL_{specs}), note that consequences may emerge greater than 4 years. In more detail: i) the sensitivity to the penetration grade

ranges from half a year to about two years (0.53 and 1.63 respectively); ii) the deeper the layer is, the higher the consequences are. Consequently, it is recommended to shorten the USL_{JMF}-LSL_{JMF} accordingly.

Importantly, for the layer FC and the indicator AV, note that: i) a range USL_{specs}-LSL_{specs} = 8% is considered; ii) for AV=LSL=18%, the expected life of the pavement is 21.3 years and the expected life of the FC is much higher; iii) for AV=USL=26%, the expected life of the friction course is would appear negligible, while the expected life of the pavement is 18.9 years because of the cement-treated failure. At the same time, if the FC were replaced, the evolution of the distress of the CT would be different and a higher expected life would be expected. Consequently, the corresponding sensitivities in Table 2 (2.34 years and 23%, respectively) are affected by this interpretation issue.

Fig. 8 summarizes the effects of P_b, gradation (AG), asphalt binder penetration (Pen), and air voids content (AV), in terms of years (ΔY) and penalties (%,ΔPA). Fig. 8 highlights how the maximum value of ΔPA is 11.35% for the case of BAC (varying $\rho_{3/4}$).

The corresponding sensitivity in terms of years is 3.59 years (ΔY). Importantly, this fact emphasizes that the specification limits in the area of the maximum aggregate size should have stricter specifications.

Conclusions and summary

Asphalt concrete contracts state that construction main variables (e.g., air voids content, AV) must comply with limits (contract specification limits, SL, USL_{specs}, LSL_{specs}). Furthermore, if a Job mix formula is approved, each variable must comply with ever narrower limits (J-specification limits, USL_{JMF}, LSL_{JMF}).

The study described in this paper deals with the assessment of the effects of these permitted variations on expected life and pay adjustment.

To this end, equation 19 and 22-24 were herein set up.

Moduli were derived through the Witczak model, the expected life of pavement by the KenPave software, and pay adjustment by equations 20 and 21. For the as-design pavement (Fig. 3), based on the proper consideration of material characteristics and traffic, an expected life of 20 years was obtained.

The method herein set up builds on mechanics even if the numerosity and complexity of interactions involves the need for a careful calibration. Based on results, the following conclusions can be drawn:

i) Usually, AV-related consequences are worse than Pen-related consequences, which, in turn, outrank AG- and P_b-related consequences. An exception is given by the maximum size of aggregates.

ii) Except that for $\rho_{3/4}$, the variations of the aggregate gradation (AG) within the JMF-specification limits (where JMF stands for job mix formula) have no relevant influence on expected life and on pay adjustment, which vary at most of ± 0.5 year and ± 1.6%, respectively. Even extending the variations of the aggregate gradation to 3 times the specification limits, the effects in terms of expected life appear irrelevant, except that for the pay adjustment of the BAC, which varies in the range [-5.2%, +4.6%] for the sieve $\rho_{3/4}$, in the range [-2.3%, +1.0%] for the sieve $P_{3/8}$, in the range [-5.1%, +5.0%] for the sieve ρ_4, and in the range [-5.2%, +0.9%] for the sieve ρ_{200}. Furthermore, the failure of the pavement is due to the CT.

iii) In terms of percentage of asphalt binder is it possible to observe that:

   a) A variation of the asphalt binder percentage of ±3 times the J-tolerance in FC, BIC and BAC implies no significant variations of EXL and PA.

   b) On the contrary, AV variations imply a sharp reduction of the EXL.

iv) Higher values of the penetration of asphalt binder in FC, BIC and BAC imply a reduction in terms of expected life and pay adjustment, according to a monotonous trend. The failure of the pavement is always due to the breaking of cement-treated layer, except when penetration of BAC asphalt binder is lower than 3 times the tolerance with respect to the as-design value. In that case the failure of the pavement is due to the BAC.

v) Variations of air voids in ± 3JT (where USL_{JMF}-LSL_{JMF}=2JT) have a strong influence on each layer. Values of AV, added of 3 times the tolerance, imply a great reduction of PA. The most critical situation occurs for the BIC, which causes the failure of the pavement in less of 2 years and reduces the PA of -92%.

vi) Sensitivity analysis confirms that AV is the most relevant parameter for the expected life and for the pay adjustment of the pavement, with an ΔY, sensitivity in years, of 2.34 years and an ΔPA, sensitivity in pay adjustment, of 23% for the FC.

vii) When contract-related limits SL_C (instead of SL_J) are considered, it turns out that consequences are severer (1-3 times greater). This originates from being C-specification limits wider than J-specification limits.

Results of this study demonstrate that small variations (i.e., ± JT) of asphalt binder content or asphalt binder penetration do not have a relevant impact on expected life and on pay adjustment. This statement is no more valid if the variations concern the air void or $\rho_{3/4}$ or if they become "high" (i.e., ± 3JT). In those cases, pavement could fail in a very short time.

Furthermore, it is assessed that when pay adjustments build on empirical algorithms, they have to be layer-specific because the same "error" implies severer consequences in deeper layers.

Further research will investigate the effect on EXL and PA varying concurrently and how the results of this investigation are affected by the design model used.

Notation list

The following symbols are used in this paper:

AG = aggregate gradation;

ANAS = ANAS contract specifications;

AV = air void content [%];

BAC = base course;

bBAC = asphalt binder percentage for the base course;

BIC = binder course;

C_{REH} = costs of successive rehabilitations [€/m^2];

C_{RES} = costs of successive resurfacings [€/m^2];

CT = sub-base (cement-treated base course);

D = 20, expected life of the as-design pavement [years];

E = E* = dynamic modulus [MPa];

|E*| = dynamic modulus [psi], (1psi = 0.0069MPa);

EBAC = dynamic modulus of the base course [MPa];

EXL = EREH = expected life of the as-constructed pavement [years];

f = loading frequency [Hz];

FC = friction course (porous asphalt concrete);

G_b = asphalt binder specific gravity;

G_{mb} = bulk specific gravity of the compacted mixture;

G_{mm} = maximum theoretical specific gravity of the mixture;

G_{sa} = apparent specific gravity of the aggregate;

G_{sb} = bulk specific gravity of the aggregate;

G_{se} = effective specific gravity of the aggregate;

I = indicator;

i = 0.04, inflation rate;

ΔPA = sensitivity of the ratio PA/C in terms of %;

ΔPA_{JMF} = sensitivity of the ratio PA/C in terms of % referred to the Job mix formula;

ΔPA_{specs} = sensitivity of the ratio PA/C in terms of % referred to contract requirements;

ΔY = sensitivity of EXL in terms of years;

ΔY_{JMF} = sensitivity of EXL in terms of years referred to the Job mix formula;

ΔY_{specs} = sensitivity of EXL in terms of years referred to contract requirements;

JMF = Job mix formula;

JT = job mix formula tolerance;

LCCA = Life Cycle Cost Analyses of the pavement;

LSL = lower specification limit;

LSL_{specs} = lower specification limit (contract requirements for the given layer);

LSL_{JMF} = lower specification limit (job mix formula);

N = compaction energy expressed in terms of number of passes with respect to the "refusal" value (0 to 1);

O = EXLFC = ERES = expected time of the as-constructed friction course (FC, typically 10 years);

P_b = asphalt content (percent by mass of total mix);

P'_b = asphalt content (percent by mass of aggregate);

$P_{3/4}$ = passing at the 3/4-inch sieve, which corresponds to 100-$\rho_{3/4}$;

$P_{3/8}$ = passing at the 3/8-inch sieve;

P_4 = passing at the 3/8-inch sieve;

PA = pay adjustment;

PA/C = $(PA_{RES}+PA_{REH})/(C_{RES}+C_{REH})$, [%];

PAC = Porous Asphalt Concrete;

PA_{REH} = pay adjustment for rehabilitation;

PA_{RES} = pay adjustment for resurfacing;

P_{ba} = percent of absorbed asphalt (by total weight of aggregate);

P_{be} = effective asphalt content [%];

Pen = asphalt binder penetration [0.1mm].

PV = present value of agency costs;

R = ratio between (1+i) and (1+r);

r, i = interest rate, inflation rate;

514 SL_{specs} = specification limit (contract requirements);

515 SL_{JMF} = specification limit (job mix formula);

516 SUB = subgrade;

517 t = thickness;

518 UB = compacted subgrade;

519 USL = upper specification limit;

520 USL_{specs} = upper specification limit (contract requirements for the given layer);

521 USL_{JMF} = upper specification limit (job mix formula);

522 V_{ba} = volume of absorbed asphalt binder [%];

523 V_{beff} = effective asphalt binder content [% by volume];

524 V_{beff} = effective asphalt binder content [% by volume];

525 α = coefficients to calibrate;

526 β = coefficients to calibrate;

527 γ = coefficients to calibrate;

528 η = asphalt binder viscosity [10^6 Poise = 10^5 Pas];

529 ρ_{200} = passing percentage the 0.075 mm (No. 200) sieve;

530 $\rho_{3/4}$ = cumulative % retained on the 19 mm (3/4 inch) sieve;

531 $\rho_{3/8}$ = cumulative % retained on the 9.5 mm (3/8 inch) sieve;

532 ρ_4 = cumulative % retained on the 4.75 mm (No. 4) sieve;

533

534

535

536 ## Data Availability Statements

537

538 Data generated or analyzed during the study are available from the corresponding author by request.

References

Al-Khateeb, G., Shenoy, A., Gibson, N., and Harman, T. (2006). "A new simplistic model for dynamic modulus predictions of asphalt paving mixtures". *Annual Meeting of Association of Asphalt Paving Technologists*, Savannah, Georgia.

ANAS Contract Specifications (2000). "Capitolato Speciale di Appalto - Parte 2ª Norme tecniche - Pavimentazioni stradali/autostradali".

Andrei, D., Witczak, M.W., Mirza, M.W. (1999). *Development of revised predictive model for the dynamic(complex) modulus of asphalt mixtures*(NCHRP 1-37A Interim Report). University of Maryland.

(13) (PDF) Evaluation of dynamic modulus of typical asphalt mixtures in Northeast US Region. Available from: https://www.researchgate.net/publication/241730997_Evaluation_of_dynamic_modulus_of_typical_asphalt_mixtures_in_Northeast_US_Region [accessed May 04 2019].

Arifin, S., Selintung, M., Samang, L. (2015). "Effect of Effective Specific Gravity on VMA Of Asphalt Concrete (Case Study of Lolioge Materials of Palu City)". *International Journal of Engineering and Technology*, Volume 5, No. 4, ISSN: 2049-3444.

Asphalt Institute (1982). *Research and Development of the Asphalt Institute's Thickness Design Manual (MS-1) Ninth Edition*, Research Report No. 82-2, The Asphalt Institute.

Boussinesq, J. (1885). *Application des potentiels a l'etude de l'equilibre et due mouvement des solids elastiques*, Gauthiers-Villars, Paris.

Bucchi, A., Costa, C., Vignali, V. (2009). "Studi preliminari per la costruzione della terza corsia". *Strade & Autostrade*, Progettazione Stradale, 3-2009.

Bulletin 27: *Bituminous Concrete Mixtures, Design Procedures, and Specifications for Special Bituminous Mixtures.* Pennsylvania Department of Transportation. Edition Change 5. Chapter 2. January 2003.

California Test Number. (2010). "Method of test for optimum binder content (OBC) for HMA type A, B, C, and RHMA-G". *California Test Number 367*, State of California – Business, Transportation and Housing Agency, Department of Transportation – Division of engineering services, Transportation Laboratory, Sacramento, California.

Cho, Y. H., Park, D. W., and Hwang, S. D. (2010). "A predictive equation for dynamic modulus of asphalt mixtures used in Korea". *Construction and Building Materials*, 24, 513–519, doi: 10.1016/j.conbuildmat.2009.10.008.

Clyne, T. R., Li, X., Marasteanu, M. O., and Skok, E. L. (2003). *Dynamic and Resilient Modulus on Mn/Dot Asphalt Mixtures*, Final Report University of Minnesota.

Colonna, P., Berloco, N., Ranieri, V., Shuler, S.T (2012). *Application of Bottom Ash for Pavement Binder Course*. Procedia - Social and Behavioral Sciences 53:962–972. DOI10.1016/j.sbspro.2012.09.945

Christensen D. W. & Bonaquist R. (2015) *Improved Hirsch model for estimating the modulus of hot-mix asphalt*, Road Materials and Pavement Design, 16:sup2, 254-274, DOI: 10.1080/14680629.2015.1077635

Cross, S. A., Jakatimath, Y., and Sumesh, K. C. (2007). *Determination of Dynamic Modulus Master Curves for Oklahoma HMA Mixtures*, Final Report FHWA/OK 07 (05), Oklahoma State University Civil & Environmental Engineering, No. AA-5-81014, 81025, 84745, 11806.

593 Esfandiarpour, S., and Shalaby, A. (2017). “Alternatives for calibration of dynamic modulus prediction models
594 of asphalt concrete containing RAP”. *International Journal of Pavement Research and Technology*, Volume
595 10, Issue 3, Pages 203-218.
596
597 Garcia, G., and Thompson, M. (2007). *HMA dynamic modulus - temperature relations,* Research Report,
598 FHWA-ICT-07-006, ISSN: 0197-9191.
599
600 Gaspard, K. J. (2000). *Evaluation of Cement Treated Base Courses*, Technical Assistance Report Number 00-
601 1TA.
602
603 Georgouli, K., Loizos, A., Plati, C., (2016). “Calibration of dynamic modulus predictive model”. *Construction*
604 *and Building Materials* 102, 65–75.
605
606 Ghadimi, B., Nikraz, H., Leek, C., and Nega, A. (2013). “A Comparison between Austroads Pavement
607 Structural Design and AASHTO Design in Flexible Pavement”. Department of Civil Engineering, Curtin
608 University, GPO Box U1987, Perth, WA 6845, Australia.
609
610 Giannattasio, P., Caliendo, C., Esposito, L., Festa, B., and Pellecchia, W. (1989). *Portanza dei sottofondi*,
611 Fondazione Politecnica per il Mezzogiorno d'Italia, Catalogo delle pavimentazioni stradali a cura del C.N.R.,
612 Gruppo di lavoro "Progettazione Pavimentazioni".
613
614 Giuliana, G., Nicolosi, V., Festa, B., (2012). “Predictive Formulas of Complex Modulus for High Air Void
615 Content Mixes”. *Transportation Research Board 91st Annual Meeting*, Washington DC, United States.
616
617 Hanifa, K., Abu-Farsakh, M. Y., and Gautreau, G. P. (2015). *Design Values of Resilient Modulus for Stabilized*
618 *and Non-Stabilized Base,* LTRC Project No. 10-3GT, State Project No. 736-99-1727, Louisiana Transportation
619 Research Center, Louisiana Department of Transportation and Development.
620

621 Hossain, N. E. I., Singh, D., and Zaman, M. (2013). "Dynamic Modulus-based Field Rut Prediction Model
622 from an Instrumented Pavement Section". *2nd Conference of Transportation Research Group of India (2nd*
623 *CTRG)*, Procedia - Social and Behavioral Sciences 104, 129 – 138, doi: 10.1016/j.sbspro.2013.11.105.
624
625 Houben, L. J. M. (2009). *Structural Design of Pavements, PART IV - Design of Concrete Pavements*.
626
627 Huang, H. Y. (2004). *Pavement Analysis and Design – Second Edition*, Pearson Education, Upper Saddle
628 River, NJ 07458, ISBN 0-13-142473-4.
629
630 Hughes, C. S., Moulthrop, J. S., Tayabji, S., Weed, R. M., and Burati, J. L. (2011). *Guidelines for quality-*
631 *related pay adjustment factors for pavement*, NCHRP Project No. 10-79.
632
633 Jung, Y. S., Zollinger, D. G., Cho, B. H., Won, M., and Wimsatt, A. J. (2012). *Subbase and subgrade*
634 *performance investigation and design guidelines for concrete pavement*, Report 0-6037-2, Project 0-6037,
635 Texas Department of Transportation and the Federal Highway Administration. Texas Transportation Institute.
636
637 Lee, K., Kim, H., Kim, N., and Kim, Y. (2002). "Dynamic Modulus of Asphalt Mixtures for Development of
638 Korean Pavement Design Guide". *Journal of Testing and Evaluation*. ASTM International, 100 Barr Harbor
639 Drive, PO Box C700, West Conshohocken, PA 14928-2959.
640
641 Leiva-Villacorta, F., Loría, L., and Aguiar-Moya, J. P. (2013). "Development of an improved and more
642 effective dynamic modulus E* model for mixtures in Costa Rica by means of artificial neural networks". *92nd*
643 *Annual Meeting of the Transportation Research Board*.
644
645 Maher, A., and Bennert, T. (2008). *Evaluation of Poisson's Ratio for Use in the Mechanistic Empirical*
646 *Pavement Design Guide (MEPDG)*, Final Report FHWA-NJ-2008-004, Dept. of Civil & Environmental
647 Engineering Center for Advanced Infrastructure & Transportation (CAIT) Rutgers, The State University
648 Piscataway, NJ, 08854-8014.

McGennis, R. B., Anderson, R. M., Kennedy, T. W., and Solaimanian, M. (1995). *Background of superpave Asphalt Mixture Design & Analysis*, Final Report, Publication No. FHWA-SA-95-003, National Asphalt Training Center Demonstration Project 101.

Molenaar, A. A. A. (2009). *Structural Design of Pavements. Part III: Design of Flexible Pavements*, CT 4860.

NCHRP Report 465. Simple Performance Test for Superpave Mix Design.

Nielsen, L.E. (1970). "Generalized Equation for the Elastic Moduli of Composite Materials". Journal of Applied Physics, Volume 41, Issue 11, p. 4626-4627.

Peinado F., Medel E., Silvestre R. and Garcia A.: *Open-grade wearing course of asphalt mixture containing ferrite for use as ferromagnetic pavement.* Composites: Part B 57 (2014) 262–268.

Pezzano, P. (2009). *La progettazione e la verifica di pavimentazioni stradali rinforzate innovative*, Tesi di Laurea in Sovrastrutture stradali e ferroviarie, Università degli Studi di Bologna, Facoltà di Ingegneria, Dipartimento di Ingegneria delle Strutture, dei Trasporti, delle Acque, del Rilevamento, del Territorio DISTART.

Popovics, J. S. (2008). *A Study of Static and Dynamic Modulus of Elasticity of Concrete*, ACI-CRC Final Report, University of Illinois, Urbana, IL.

Praticò, F. G. (2016). "A Few Dilemmas Pertaining Transportation Infrastructures and Their Sustainability". *Sustainability Issues in Civil Engineering*, pp: 15-33.

Praticò, F. G., Noto, S., and Astolfi, A. (2016). "Issues and perspectives in the application of different pavement design methods to life cycle cost analysis". *Proc. of the Eighth Intl. Conf. on Maintenance and*

Rehabilitation of Pavements, Mairepav8, Published by Research Publishing, Singapore, ISBN: 978-981-11-0449-7, doi:10.3850/978-981-11-0449-7-083-cd.

Putri, E. E., Kameswara Rao, N. S. V., Mannan, M. A. (2012). "Evaluation of Modulus of Elasticity and Modulus of Subgrade Reaction of Soils Using CBR Test". *Journal of Civil Engineering Research*, 2(1): 34-40, doi: 10.5923/j.jce.20120201.05.

Riccardi, C. (2017). *Mechanistic modelling of bituminous mortars to predict performance of asphalt mixtures containing rap*, University of Florence, Italy.

Rojas, J., Nazarian, S., Tandon, V., and Yuan, D. (1998). "Quality management of asphalt-concrete layers using wave propagation techniques". *AAPT Annual Meeting*, Reports/RPA_A1698.

Seo, J., Kim, Y., Cho, J., and Jeong, S. S. (2013). "Estimation of in situ dynamic modulus by using MEPDG dynamic modulus and FWD data at different temperatures". *International Journal of Pavement Engineering*, Vol. 14, No. 4, 343–353, Doi: 10.1080/10298436.2012.664274.

Shahadan, Z., Hamzah, M.O, Yahya, A.S., and Jamshidi, A. (2013). *Evaluation of the dynamic modulus of asphalt mixture incorporating reclaimed asphalt pavement*. Indian Journal of Engineering & Materials Sciences. Vol 20, pp 376 – 384.

Sukirman, S. (2010). *The Hot Mix of Asphalt Concrete*, Granit, Yogyakarta.

Walls, J., and Smith M. R. (1998). *Life-Cycle Cost Analysis*, Pavement Division, HNG-40 Office of Engineering - Federal Highway Administration 400 7th Street SW, Washington, DC 20590.

WAQTC TM 13 (2012). *Volumetric Properties of Hot Mix Asphalt (HMA)*.

705 Witczak, M. W., and Fonseca O. A. (1996). "Revised Predictive Model for Dynamic (Complex) Modulus of
706 Asphalt Mixtures". *Transportation Research Record*, 1540, pp. 15-23.
707
708 Wu, Z., Yangb, X., Sun, X., (2017). "Application of Monte Carlo filtering method in regional sensitivity
709 analysis of AASHTO Ware Pavement ME design". *Journal of Traffic and Transportation Engineering*
710 *(English Edition)*, 4 (2): 185-197.
711
712 Xiao, Y. (2009). *Evaluation of Engineering Properties of Hot Mix Asphalt Concrete for the Mechanistic*
713 *Empirical Pavement Design*, Electronic Theses, Treatises and Dissertations. Florida State University Libraries.
714
715 Yousefdoost, S., Vuong, B., Rickards, I., Armstrong, P., and Sullivan, B. (2013). "Evaluation of Dynamic
716 Modulus Predictive Models for Typical Australian Asphalt Mixes". *15th International Flexible Pavements*
717 *Conference.*
718
719 Yu, J. (2012). *Modification of Dynamic Modulus Predictive Models for Asphalt Mixtures Containing Recycled*
720 *Asphalt Shingles*, Jowa State University.
721

Figures

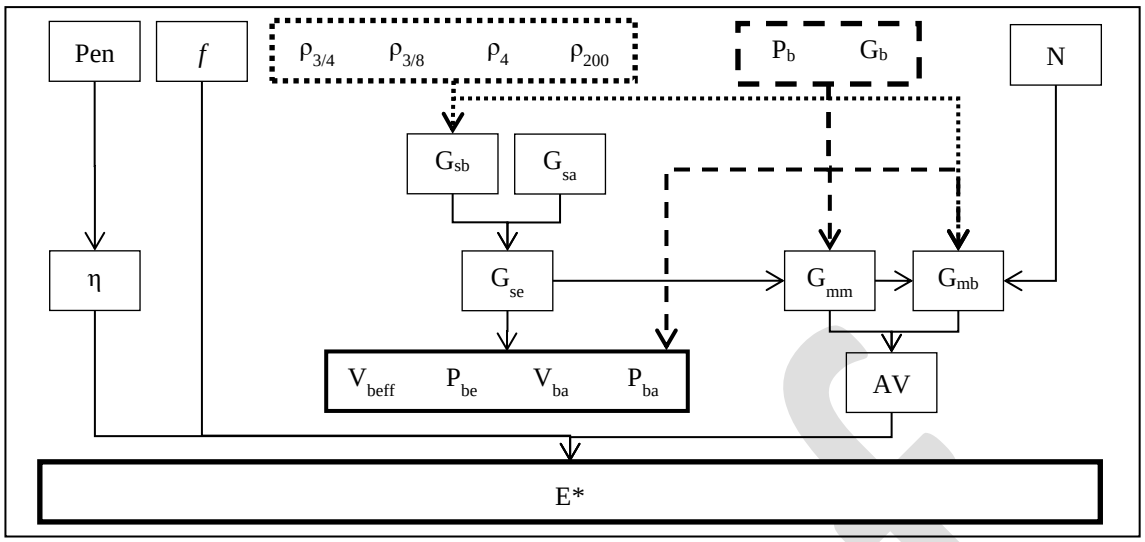

Fig. 1. Main variables that affect a bituminous layer modulus

Symbols. ρ_{200}: % Passing the 0.075 mm (No. 200) sieve; ρ_4: Cumulative % retained on the 4.75 mm (No. 4) sieve; $\rho_{3/8}$: Cumulative % retained on the 9.5 mm (3/8 inch) sieve; $\rho_{3/4}$: Cumulative % retained on the 19 mm (3/4 inch) sieve; *f*: Loading frequency [Hz]; Pen: asphalt binder penetration [0.1 mm]; η: asphalt binder viscosity [10^6 Poise]; P_b: Asphalt content (percent by mass of total mix); G_b: Asphalt binder specific gravity; G_{mb}: Bulk specific gravity of the compacted mixture; G_{sb}: Bulk specific gravity of the aggregate; G_{sa}: Apparent specific gravity of the aggregate; G_{se}: Effective specific gravity of the aggregate; G_{mm}: Maximum theoretical specific gravity of the mixture; P_{ba}: Percent of absorbed asphalt (by total weight of aggregate); P_{be}: Effective asphalt content [%]; AV: Air void content [%]; V_{beff}: Effective asphalt binder content [% by volume]; V_{ba}: Volume of absorbed asphalt binder [%]; E*: Dynamic modulus; N: compaction energy (in percentage with respect to the maximum value).

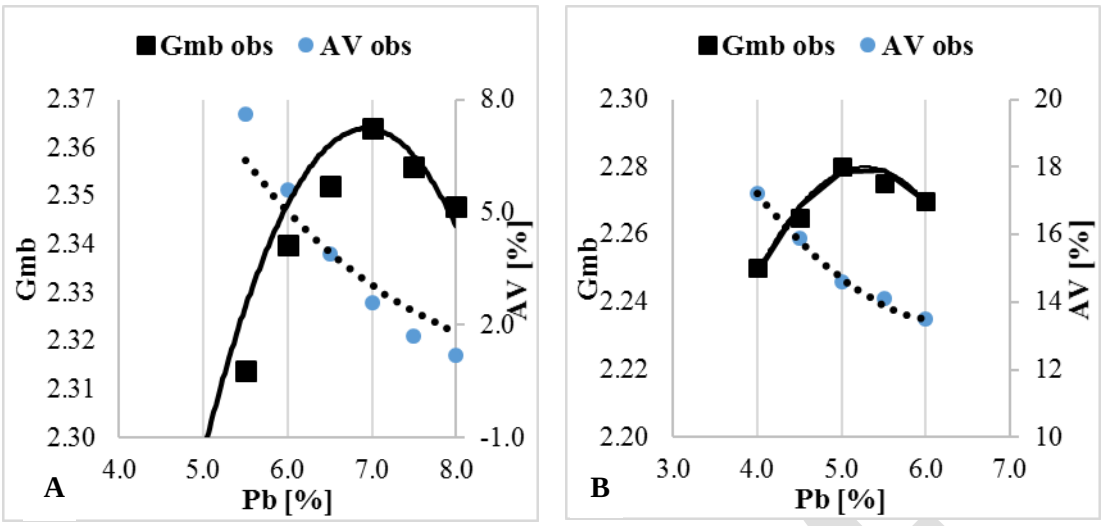

Fig. 2. Example of prediction of AV and Gmb based on eq. 19 for a dense-graded mix (A) and an open-graded mix (B).

Symbols. AV: air content; AVobs: observed values of air content, Pb: Asphalt content (percent by mass of total mix); Gmb: Bulk specific gravity of the compacted mixture; Gmbobs: observed values of bulk specific gravity of the compacted mixture.

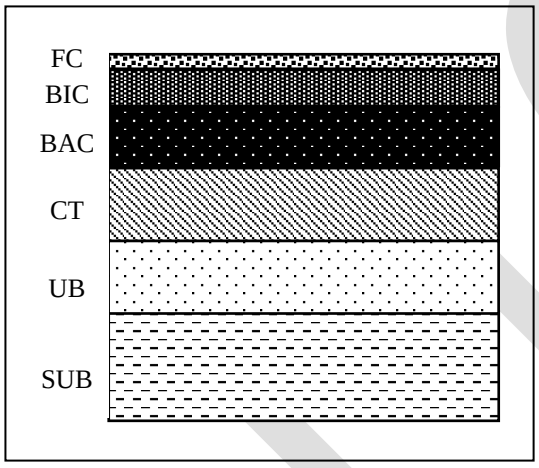

Fig. 3. As design pavement (scheme)

Symbols. FC: friction course (porous asphalt concrete); BIC: binder course; BAC: base course; CT: sub-base (cement-treated base course); UB: compacted subgrade; SUB: subgrade; E: dynamic modulus; t: thickness.

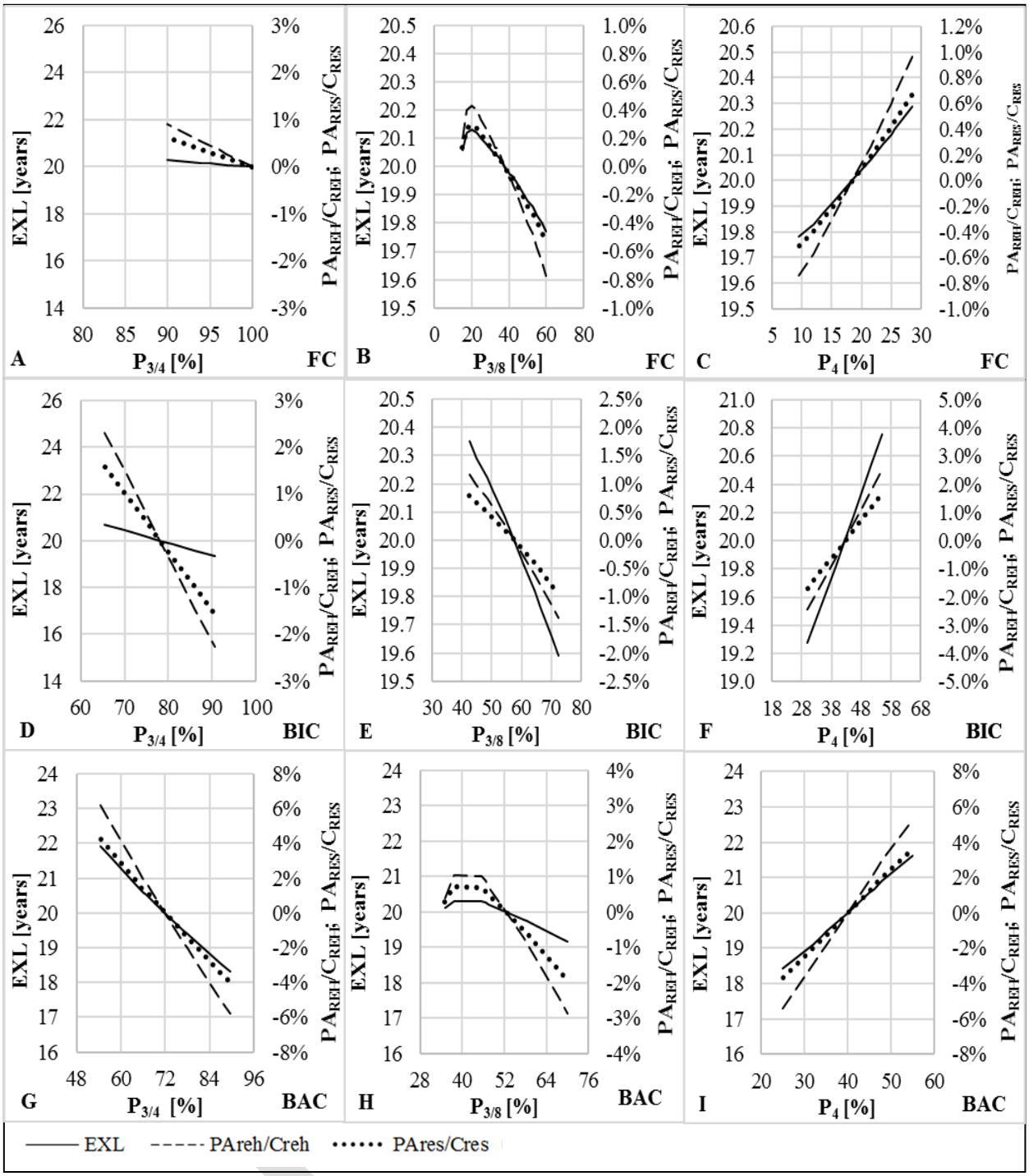

754

755 **Fig. 4**. EXL and PA vs $P_{3/4}$ (A, D, G), $P_{3/8}$ (B, E, H), P_4 (C, F, I) for FC, BIC, and BAC

756 Symbols. $P_{3/4}$, $P_{3/8}$, P_4: percent passing to the given sieve; FC: friction course; BIC: binder course; BAC: base course;

757 EXL = expected life; PA_{REH}, PA_{RES}: pay adjustment for rehabilitation and resurfacing, respectively. C_{REH}, C_{RES}: costs.

758

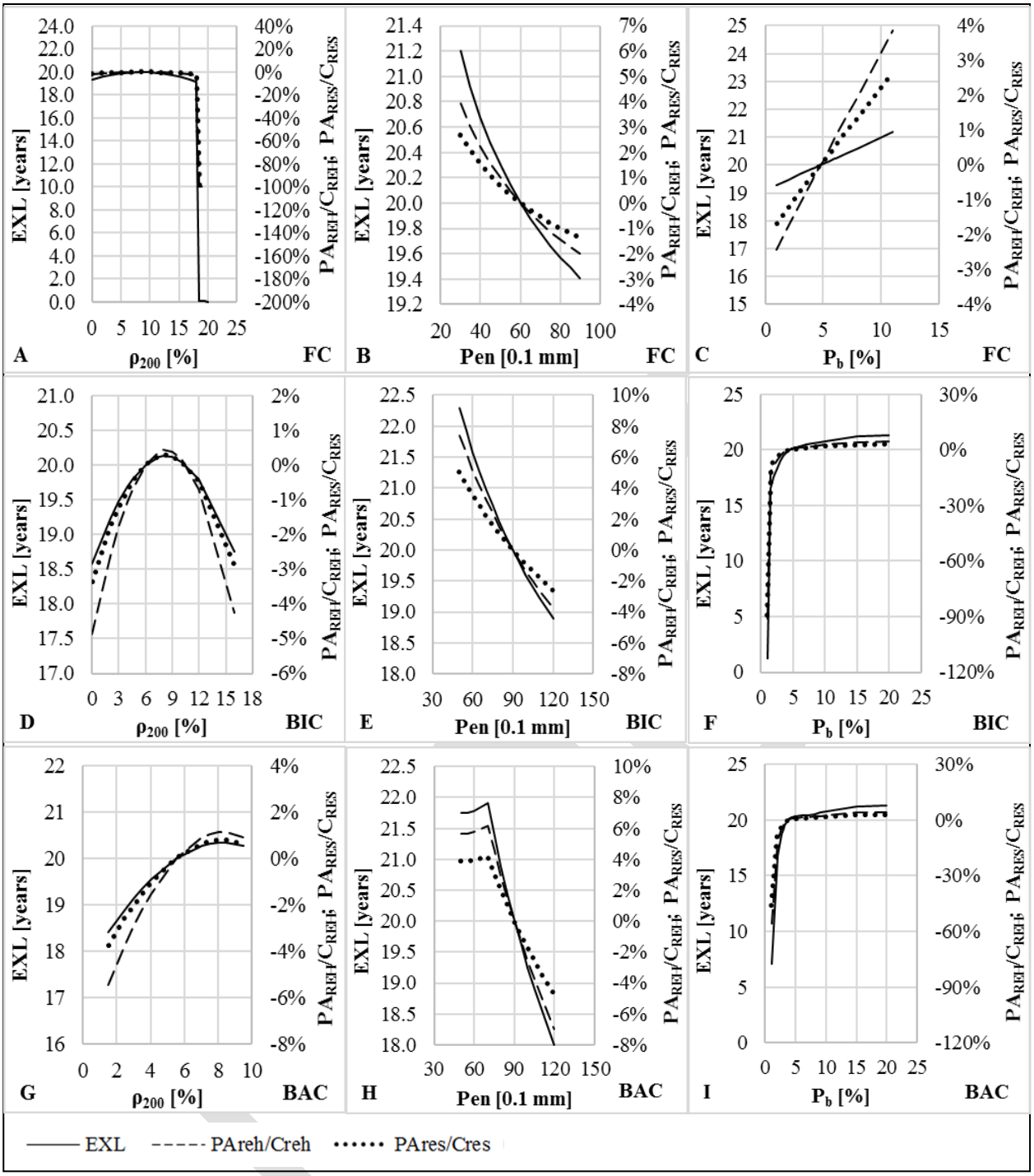

Fig. 5. EXL and PA vs ρ_{200} (A), Pen (B), P_b (C) for FC, BIC, and BAC

Symbols. ρ_{200}: passing; Pen: penetration; P_b: bitumen percentage; FC: friction course; BIC: binder course; BAC: base course; EXL = expected life; PA_{REH}, PA_{RES}: pay adjustment for rehabilitation and resurfacing, respectively. C_{REH}, C_{RES}: costs.

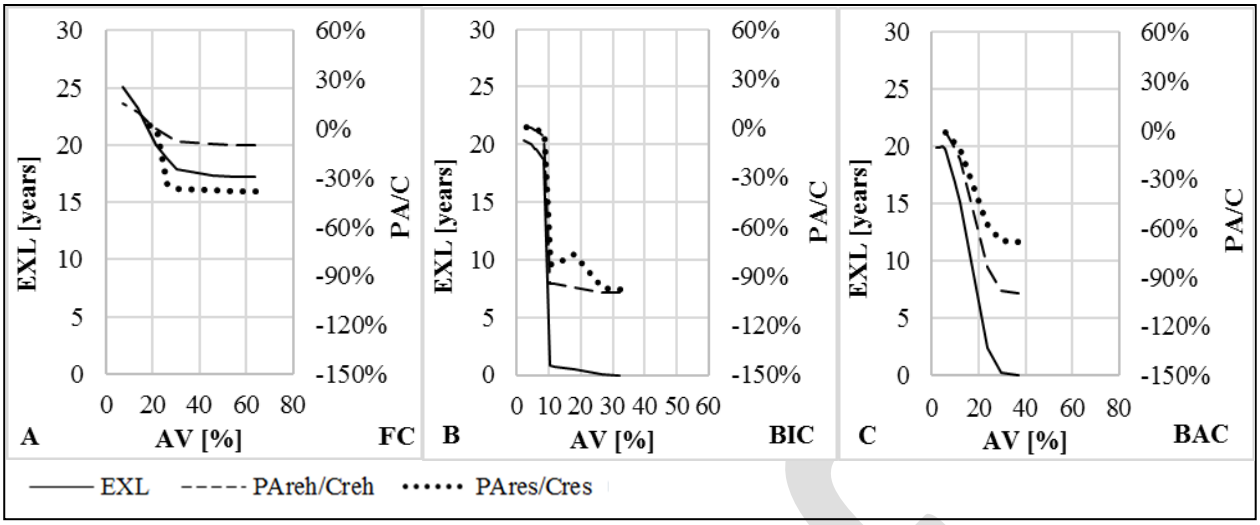

765

766 **Fig. 6.** EXL and PA vs AV (air voids) for FC, BIC, and BAC

767 Symbols. AV: air content; FC: friction course; BIC: binder course; BAC: base course; EXL = expected life; PA_{REH},

768 PA_{RES}: pay adjustment for rehabilitation and resurfacing, respectively. C_{REH}, C_{RES}: costs.

769

770

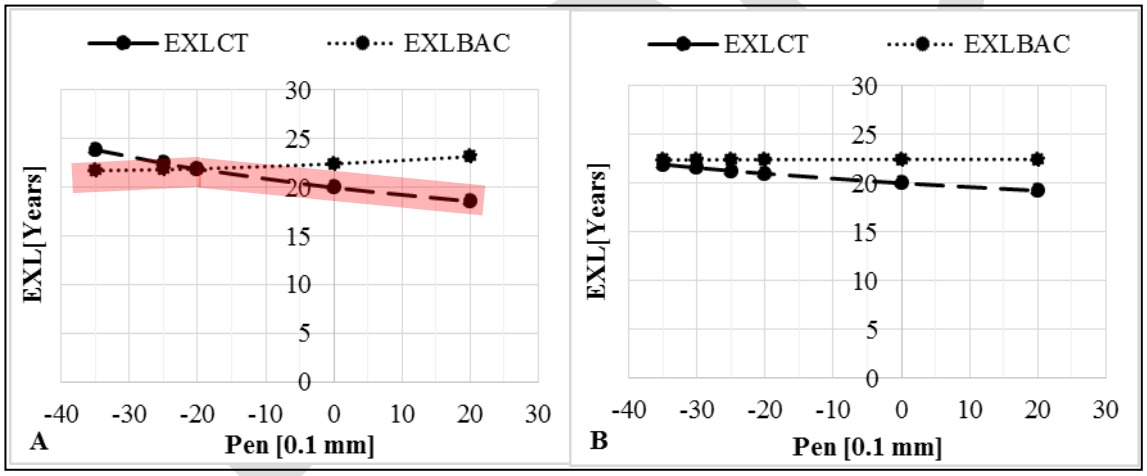

771

772 **Fig. 7.** Consequences of BAC (A) and BIC (B) nonconformity on the expected life of the pavement

773 Symbols. EXLCT = expected life of sub-base (cement-treated base course); EXLBAC = expected life of base course;

774 Pen: penetration.

775

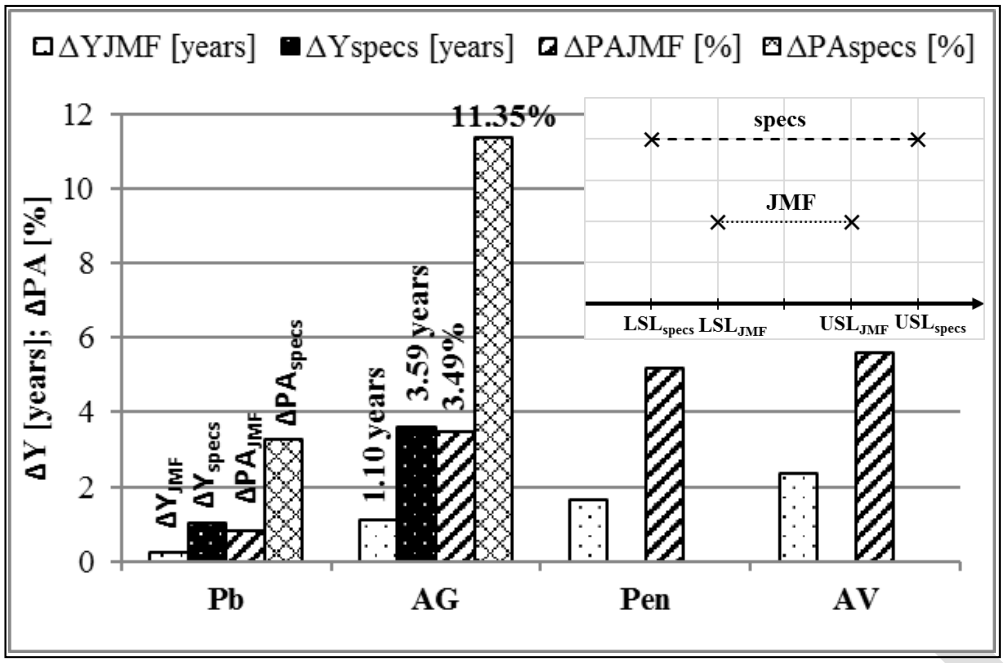

776

777 **Fig. 8.** Sensitivity of expected life (ΔY) and PA (ΔPA) to variations within specification limits type JMF or

778 type specs

779 Symbols. EXL = expected life; PA_{REH}, PA_{RES}: pay adjustment for rehabilitation and resurfacing, respectively. C_{REH},

780 C_{RES}: costs; ΔY_{JMF} = sensitivity of EXL in terms of years referred to the Job mix formula; ΔY_{specs} = sensitivity

781 of EXL in terms of years referred to contract requirements; ΔPA_{JMF} = sensitivity of the ratio PA/C in terms of

782 % referred to the Job mix formula; ΔPA_{specs} = sensitivity of the ratio PA/C in terms of % referred to contract

783 requirements; P_b = asphalt binder content; AG: gradation; Pen = asphalt binder penetration; AV = air void

784 content.

785

786

787 ## Table

788 **Table 1:** Layers moduli

Layer	**Reference value** E (MPa)	**Reference value** t (cm)	**Design value** E (MPa)	**Design value** t (cm)
Friction course (FC)	448[a] ÷ 2258[b]	-	1013	5
Binder course (BIC)	2188[c] ÷ 8220[d]	4[e] ÷ 9[e]	4393	7
Base course (BAC)	3085[c] ÷ 9418[d]	7[e] ÷25[e]	5101	15
Sub-base (CT)	1263[f] ÷ 1583[g]	-	1423	20
Compacted Subgrade (UB)	160[h] ÷ 491[h,i]	20[l] ÷ 30[l]	252	20
Subgrade (SUB)	45[m] ÷ 242[m]	semi-inf[n]	85	semi-inf

Note: FC = friction course (porous asphalt concrete); BIC = binder course; BAC = base course; CT = sub-base (cement-treated base course); UB = compacted subgrade; SUB = subgrade; E = dynamic modulus; t = thickness.
[a]based on Cho et al. 2010.
[b]based on Asphalt Institute 1982.
[c]based on Leiva-Villacorta et al. 2013.
[d]based on Witczak and Fonseca 1996.
[e]based on reference data.
[f]based on Gaspard 2000.
[g]based on Molenaar 2009.
[h]based on Giannattasio et al. 1989.
[i]based on Hossain et al. 2013.
[l]based on Bucchi et al. 2009.
[m]based on Putri et al. 2012.
[n]based on Boussinesq 1885.

Table 2: Sensitivity of EXL and PA/C for each parameter and layer

	Indicator →	$\rho_{3/4}$		$\rho_{3/8}$		ρ_4		ρ_{200}		P'_b		Pen	AV
	↓ Layer ↓	SL_{JMF}	SL_{specs}	SL_{JMF}	SL_{specs}	SL_{JMF}	SL_{specs}	SL_{JMF}	SL_{specs}	SL_{JMF}	SL_{specs}	SL_{specs}	SL_{specs}
Range of variation of I	FC	0.0±3.0	0.0±0.0	62.5±3.0	62.5±22.5	81.5±3.0	81.5±6.5	10.0±1.5	10.0±2.0	5.00±0.25	5.00±0.50	60±10	22.0±4.0
	BIC	22.0±3.0	22.0±18.5	42.5±3.0	42.5±12.5	57.5±3.0	57.5±12.5	6.0±1.5	6.0±2.0	4.50±0.25	4.50±0.50	90±10	5.9±2.9
	BAC	28.0±5.0	28.0±18.0	47.5±5.0	47.5±17.5	60.0±5.0	60.0±15.0	5.5±1.5	5.5±2.5	3.75±0.25	3.75±0.75	90±10	5.5±2.5
$\Delta Y'$	FC	0.08	-	0.06	0.33	0.16	0.35	0.11	0.14	0.08	0.15	0.53	2.34
	BIC	0.33	-	0.16	0.63	0.36	1.48	0.32	0.44	0.21	0.43	0.87	1.60
	BAC	1.02	3.59	0.43	1.15	1.10	3.19	0.73	1.20	0.25	1.02	1.63	1.71
ΔPA (%)	FC	0.25	-	0.19	1.05	0.51	1.11	0.35	0.44	0.25	0.48	1.68	22.62
	BIC	1.02	-	0.51	2.00	1.14	4.69	1.02	1.40	0.50	1.37	2.76	5.18
	BAC	3.24	11.35	1.36	3.69	3.49	10.11	2.32	3.80	0.80	3.27	5.16	5.60

Note: ΔY = sensitivity of EXL; ΔPA = sensitivity of PA/C; ρ_{200} = passing the 0.075 mm (No. 200) sieve; ρ_4 = cumulative % retained on the 4.75 mm (No. 4) sieve; $\rho_{3/8}$ = cumulative % retained on the 9.5 mm (3/8 inch) sieve; $\rho_{3/4}$ = cumulative % retained on the 19 mm (3/4 inch) sieve; Pen = penetration of a standard needle of 100 g, which penetrates the asphalt binder for 5 seconds (0.1 mm); P'_b = asphalt content (percent by mass of aggregate); AV = air void content (%); FC = friction course; BIC = binder course; BAC = base course; SLspecs = specification limit referred to contract requirements, ANAS contract specifications 2000; SL_{JMF} = specification limit referred to the job mix formula, ANAS contract specifications 2000.

List of figure captions

Fig. 1. Main variables that affect a bituminous layer modulus.

Symbols. ρ_{200}: % Passing the 0.075 mm (No. 200) sieve; ρ_4: Cumulative % retained on the 4.75 mm (No. 4) sieve; $\rho_{3/8}$: Cumulative % retained on the 9.5 mm (3/8 inch) sieve; $\rho_{3/4}$: Cumulative % retained on the 19 mm (3/4 inch) sieve; *f*: Loading frequency [Hz]; Pen: asphalt binder penetration [0.1 mm]; η: asphalt binder viscosity [10^6 Poise]; P_b: Asphalt content (percent by mass of total mix); G_b: Asphalt binder specific gravity; G_{mb}: Bulk specific gravity of the compacted mixture; G_{sb}: Bulk specific gravity of the aggregate; G_{sa}: Apparent specific gravity of the aggregate; G_{se}: Effective specific gravity of the aggregate; G_{mm}: Maximum theoretical specific gravity of the mixture; P_{ba}: Percent of absorbed asphalt (by total weight of aggregate); P_{be}: Effective asphalt content [%]; AV: Air void content [%]; V_{beff}: Effective asphalt binder content [% by volume]; V_{ba}: Volume of absorbed asphalt binder [%]; E*: Dynamic modulus; N: compaction energy (in percentage with respect to the maximum value).

Fig. 2. Example of prediction of AV and Gmb based on eq. 19 for a dense-graded mix (A) and an open-graded mix (B)

Symbols. AV: air content; AV exp: experimental values of air content, Pb: Asphalt content (percent by mass of total mix); Gmb: Bulk specific gravity of the compacted mixture; Gmb exp: experimental values of bulk specific gravity of the compacted mixture.

Fig. 3. As design pavement (scheme).

Symbols. FC: friction course (porous asphalt concrete); BIC: binder course; BAC: base course; CT: sub-base (cement-treated base course); UB: compacted subgrade; SUB: subgrade; E: dynamic modulus; t: thickness.

Fig. 4. EXL and PA vs $P_{3/4}$ (A), $P_{3/8}$ (B), P_4 (C) for FC, BIC, and BAC.

Symbols. P3/4, P3/8, P4: percent passing to the given sieve; FC: friction course; BIC: binder course; BAC: base course; EXL = expected life; PAREH, PARES: pay adjustment for rehabilitation and resurfacing, respectively. CREH, CRES: costs.

Fig. 5. EXL and PA vs ρ_{200} (A), Pen (B), P_b (C) for FC, BIC, and BAC.

Symbols. ρ_{200}: passing; Pen: penetration; P_b: bitumen percentage; FC: friction course. EXL = expected life; PA_{REH}, PA_{RES}: pay adjustment for rehabilitation and resurfacing, respectively. C_{REH}, C_{RES}: costs.

Fig. 6. EXL and PA vs AV (air voids) for FC, BIC, and BAC

Symbols. AV: air content; FC: friction course. EXL = expected life; PA_{REH}, PA_{RES}: pay adjustment for rehabilitation and resurfacing, respectively. C_{REH}, C_{RES}: costs.

Fig. 7. Consequences of BAC (A) and BIC (B) nonconformity on the expected life of the pavement

Symbols. EXLCT = expected life of sub-base (cement-treated base course); EXLBAC = expected life of base course; Pen: penetration.

.

Fig. 8. Sensitivity of expected life (ΔY) and PA (ΔPA) to variations within specification limits type JMF or type specs

Symbols. EXL = expected life; PA_{REH}, PA_{RES}: pay adjustment for rehabilitation and resurfacing, respectively. C_{REH}, C_{RES}: costs; ΔY_{JMF} = sensitivity of EXL in terms of years referred to the Job mix formula; ΔY_{specs} = sensitivity of EXL in terms of years referred to contract requirements; ΔPA_{JMF} = sensitivity of the ratio PA/C in terms of % referred to the Job mix formula; ΔPA_{specs} = sensitivity of the ratio PA/C in terms of % referred to contract requirements; P_b = asphalt binder content; AG: gradation; Pen = asphalt binder penetration; AV = air void content.

Table 1: Layers moduli.

Symbols: FC = friction course (porous asphalt concrete); BIC = binder course; BAC = base course; CT = sub-base (cement-treated base course); UB = compacted subgrade; SUB = subgrade; E = dynamic modulus; t = thickness.

Table 2: Sensitivity EXL and PA/C for each parameter and layer.

Symbols: **ΔY** = sensitivity of EXL to I; **Δ**PA = sensitivity of PA/C to I; ρ200 = passing the 0.075 mm (No. 200) sieve; ρ4 = cumulative % retained on the 4.75 mm (No. 4) sieve; ρ3/8 = cumulative % retained on the 9.5 mm (3/8 inch) sieve; ρ3/4 = cumulative % retained on the 19 mm (3/4 inch) sieve; Pen = penetration of a standard needle of 100 g, which penetrates the asphalt binder for 5 seconds (0.1 mm); P'b = asphalt content (percent by mass of aggregate); AV = air void content (%); FC = friction course; BIC = binder course; BAC = base course; SLC = specification limit referred to

853 contract requirements, ANAS contract specifications 2000; SLJ = specification limit referred to the job mix formula,

854 ANAS contract specifications 2000.